Development of a biocompatible, low-cost reinforcement of methacrylated alginate hydrogels using synthetic crosslinking agents

Carolina Gutierrez Cisneros [a], Hannah Agten [a,b], Elien Derveaux [c], Peter Adriaensens [c], Veerle Bloemen [a,b], Arn Mignon [a,*]

[a] Department of Materials Engineering, Surface, and Interface Engineered Materials (SIEM), KU Leuven, Group T Leuven Campus, Leuven, Belgium
[b] Prometheus, Division of Skeletal Tissue Engineering, Skeletal Biology and Engineering Research Center, KU Leuven, Leuven, Belgium
[c] Analytical and Circular Chemistry (ACC), NMR group, Institute for Materials Research (imo-imomec), Hasselt University, Agoralaan, 3590 Diepenbeek, Belgium

ARTICLE INFO

Keywords:
Reinforced hydrogel
Natural-based
Biocompatible
Cost-effective

ABSTRACT

The skin is a vital organ that protects the human body, making it highly susceptible to injury. When wounds fail to heal properly, they can become chronic and prone to infection. Hydrogel-based wound dressings, made from natural and synthetic polymers, play a crucial role in wound management by enhancing the wound environment, providing a protective interface over the wound, retaining moisture, and facilitating ease of removal which supports the formation of new tissue. Among these, methacrylated alginate hydrogels show promising biological potential but require improvement in mechanical strength to meet clinical demands due to their large moisture uptake capacity. In this study, methacrylated alginate hydrogels were reinforced with four low-cost (meth)acrylic crosslinkers: ethylene glycol diacrylate, ethylene glycol dimethacrylate, triethylene glycol dimethacrylate and pentaerythritol triacrylate, to improve mechanical properties without compromising biological efficacy. The best formulation, using the first one, demonstrated a swelling capacity of 40 g of water per g of hydrogel, significantly outperforming commercial products like Kaltostat (25 g/g) and AquacelAg (18 g/g). Its mechanical strength (~0.06 MPa) was comparable to DuoDERM-ET (0.07 MPa) and Mepilex (~0.05 MPa). The hydrogel also demonstrated excellent in vitro biocompatibility, positioning it as a simple, cost-effective alternative to reinforce methacrylated hydrogels so they eventually become possibly useful as wound dressings, mechanically and physically strongly competing with commercial dressings, while still offering room for future bioactive development to enhance wound healing.

1. Introduction

The skin, the human body's largest organ, protects internal organs making it highly susceptible to injury by chemical, physical, and biological agents. Wounds are classified as acute or chronic. Acute wounds typically heal within 1–12 weeks, while chronic ones are delayed due to underlying conditions such as diabetes, or venous insufficiency, making them more difficult to treat and prone to infection [1–3]. Chronic wounds are particularly challenging due to poor healing; consequently, there is a continuous search for wound dressings that not only promote healing, but also prevent further damage. Such a treatment must absorb excess exudate while maintaining a moist environment, which can speed recovery by up to five times. Moreover, removable wound dressings are often changed regularly, such as every 1–3 days, to ensure optimal healing [4]. Biopolymer-based hydrogels are ideal for this, as they regulate moisture and create a healing environment [1,5,6].

With a backbone made of crosslinked natural and/or synthetic hydrophilic polymers, hydrogels are three-dimensional networks capable of absorbing biological fluids while preserving their structure. Their high-water content, porosity, and biocompatibility make them similar to the extracellular matrix of skin, supporting wound healing. Additionally, they are biodegradable and non-toxic, which has made them increasingly relevant in the market [2,6].

Polysaccharides, like sodium alginate (SA), are commonly used in hydrogel preparation, but their instability makes them unsuitable for wound dressings without modification. To address this, they are often grafted through the reaction of their functional groups (i.e. -OH, —COOH and -NH_2) for covalent crosslinking, resulting in stable bonding [1,2,7,8]. Sodium alginate (SA) is a widely utilized polysaccharide due to its low environmental impact and cost-effectiveness. Comprising

* Corresponding author.
E-mail address: arn.mignon@kuleuven.be (A. Mignon).

https://doi.org/10.1016/j.reactfunctpolym.2025.106330
Received 2 December 2024; Received in revised form 17 April 2025; Accepted 7 May 2025
Available online 12 May 2025

irregular blocks of β-D-mannuronic acid (M) and 1–4 linked α-L-guluronic acid (G), it can form gels via ionic crosslinking in mild environments, but its mechanical properties are insufficient for advanced wound healing applications. By grafting acrylate or methacrylate groups onto the polymer backbone, SA can undergo photocrosslinking via the carbon-carbon double bond [8], creating alginate methacrylate (ALMA). ALMA hydrogels are widely used in biomedical applications due to their enhanced mechanical properties [1,2,7,8].

The mechanical properties of ALMA hydrogels are influenced by a range of factors, including initiator concentration, UV exposure, and the degree of methacrylation (the ratio of methacrylate groups introduced to the original functional groups on the alginate backbone). Among the methods for introducing this functionality, modification with methacrylic anhydride (MAAH) is one of the most cost-effective approaches under mild conditions with few by-products [9]. However, despite improved stability through covalent crosslinking, ALMA hydrogels still lack the mechanical strength required for wound healing. Synthetic polymers can reinforce these materials but may reduce biocompatibility, while natural additives, though non-toxic, often fail to provide adequate mechanical reinforcement or are not cost-effective. Achieving a balance between mechanical strength, biocompatibility, and cost is crucial for producing hydrogels that are both effective and economically viable for clinical translation [9].

Existing commercial dressings often fail to offer an optimal compromise in terms of sufficient mechanical properties, fluid uptake, biocompatibility, and/or cost. Although previous studies have reported mechanical reinforcement of ALMA hydrogels using various crosslinking strategies [8,9], much of this research has focused on single crosslinker systems [10], non-covalent interactions [11,12] or unfunctionalized polymer hydrogels [13]. In contrast, direct comparisons between structurally distinct (meth)acrylic crosslinkers remain limited, highlighting the need for broader evaluation. The novelty of this study lies in the targeted comparison of low-cost synthetic (meth)acrylic crosslinkers, selected for their ability to covalently interact with the methacrylated functionality of alginate hydrogels (ALMA), aiming to enhance mechanical performance without compromising biocompatibility or affordability, aspects that remains underexplored in the literature, especially in relation to different crosslinker structures.

This study aimed to improve the mechanical properties of covalently crosslinked ALMA hydrogels while maintaining their biological performance and cost-effectiveness. It was done by comparing the effect of the addition of four synthetic crosslinkers in a 2:1 M ratio to the methacrylated alginate in terms of their crosslinkable functionalities. The studied molecules were ethylene glycol diacrylate (EGDA), ethylene glycol dimethacrylate (EGDMA), triethylene glycol dimethacrylate (TEGDMA) and pentaerythritol triacrylate (PETA). The focus of this study was on optimizing hydrogel formulations to enhance their physico-chemical and mechanical properties. Once these characteristics were established, subsequent research addressed biocompatibility and cost-effectiveness. Future work would then explore the incorporation of active compounds into the developed platform to support wound healing. Altogether, the presented findings provide a foundation for the development of mechanically robust and adaptable hydrogel systems with potential for clinical use in wound care.

2. Materials and methods

SA, MAAH and phosphate buffered saline (PBS) were bought from Sigma Aldrich Belgium. The photoinitiator 2-methyl-1-[4-(hydroxyethoxy)phenyl]-2-methyl-1-propanone (Irgacure® 2959, I2959), EGDMA and TEGDMA from TCI Europe. Maximum recovery diluent (MRD), peptone salts solution and fetal bovine serum (FBS, from American origin) were bought from VWR Belgium. PETA, sodium hydroxide, LIVE/DEAD Viability/Cytotoxicity Kit L-3224, bovine serum albumin (BSA), antibiotic antimycotic (AA), dimethyl sulfoxide (DMSO) and phosphate buffer saline (PBS) were bought from Fisher Scientific Belgium. EGDA was purchased from Acros Organics Belgium. Dialysis membranes Spectra/Por® 4 (MWCO 12–14 kD) were bought from Spectrum Laboratories Inc., USA. Normal Human Dermal Fibroblasts, Adult (NHDF-Ad) were bought from Lonza Belgium and granted an ethical permit approval number S67135 by the Ethical Research Commission UZ/KU Leuven. Dulbecco's Modified Eagle Medium (DMEM) high glucose GlutaMAX was bought from Life Technologies Europe. The 3-[4,5-dimethylthiazol-2-yl]-2,5 diphenyl tetrazolium bromide (MTT) cell proliferation and cytotoxicity kit was bought from Bio Connect Diagnostics, Netherlands.

2.1. Alginate methacrylation

The derivatization with MAAH was performed as described earlier [14,15]. Briefly, MAAH was added dropwise to a 2 mol% sodium alginate solution in demineralized water. The amount corresponded to 2 equivalents of MAAH per mol hydroxyl moieties on alginate. During the synthesis, released methacrylic acid lowers the pH, so it was increased and kept at pH 8 by the dropwise addition of 5 M sodium hydroxide (NaOH) solution. This light alkaline environment is maintained to increase the reaction efficiency. However, pH should not be too high to avoid the hydrolysis of the ester. The mixture was stirred at room temperature for 24 h, then purified by dialysis against distilled water with two changes per day for 3 days. The resulting modified alginate solution was dried by lyophilization (Christ freeze-dryer alpha 2–4-LSC, Martin Christ, Germany). The degree of methacrylation, also called degree of substitution (DS), was calculated with ^{1}H NMR analysis with D_2O as solvent [16].

2.2. Sample overview

The samples described in Table 1 were prepared for mechanical, physical, and biological testing ($n \geq 3$). The hydrogels containing crosslinkers are compared to a control, which is a hydrogel with only ALMA. Each of the other compositions had the same amount of ALMA but additionally one of the studied crosslinkers. The samples that could be compared according to their chemical structure (one parameter at a time) are indicated in the last column of Table 1.

To determine an optimal crosslinker ratio that enhanced mechanical properties while minimizing crosslinker addition, two molar ratios of crosslinking moieties in the crosslinker to functionalized crosslinking moieties in the alginate were tested: 1:1 and 2:1. The selection of these ratios was based on the available functional groups in the methacrylated alginate (ALMA), ensuring efficient covalent bonding while minimizing excess crosslinker. This indicates a trade-off between fluid uptake and mechanical strength, which depends on the density of covalent bonds formed. Preliminary tests with the 1:1 ratio, conducted as part of an initial screening, did not show a significant change in hydrogel properties. Therefore, the focus of this study shifted to the 2:1 ratio, which was further evaluated with four different crosslinkers. Their performance was assessed through swelling behavior, gel fraction, and mechanical testing, leading to the selection of the best-performing formulation for subsequent biocompatibility testing in cell culture.

2.3. Crosslinking

The different hydrogels were made at 5 *w/v* % of functionalized biopolymer in 10 ml deionized water. For the samples with an additional crosslinker, it was mixed based on a 2:1 (meth)acrylate molar ratio to ALMA according to the number of introduced alkene functionalities measured with ^{1}H NMR (the DS). Subsequently, an aqueous solution of Irgacure® 2959 initiator was added to the polymer solution in a concentration of 8 mol% relative to the calculated DS. The samples were protected from light with aluminum foil, mixed thoroughly with a SpeedMixer® DAC 150 (Hauschild, Germany). Then, injected between two parallel glass plates covered with a sheet of teflon foil and separated

Table 1
Sample overview of the study.

Name	ALMA	2:1 (meth)acrylate functionality molar ratio of crosslinker to ALMA		Compared to
ALMA	5 wt%	N/A		EGDA, EGDMA TEGDMA, PETA
EGDA		Ethylene glycol diacrylate	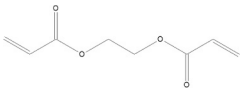	ALMA, EGDMA, PETA
EGDMA		Ethylene glycol dimethacrylate	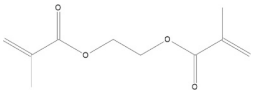	ALMA, TEGDMA
TEGDMA		Triethylene glycol dimethacrylate	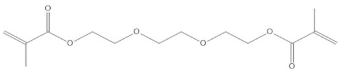	ALMA, EGDMA
PETA		Pentaerythritol triacrylate	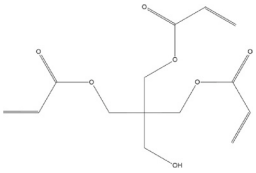	ALMA, EGDA

The added crosslinker corresponds to ~0.1 wt%.

by a 1 mm thick silicone spacer. Finally, they were placed to crosslink for an hour between two series of lamps at 365 nm (UV-A LED Gen 2 Emitter LZ1-00UV00, with a radiant flux of 800 mW at 2.8 W power dissipation).

Crosslinked hydrogels were characterized both structurally by FTIR spectrophotometer and morphologically by scanning electron microscope (SEM). Fourier transform infrared (FT-IR) spectra were recorded on freeze dried samples using a Spectrum 100 from PerkinElmer in transmission mode in the range 2000–600 cm^{-1}. High-resolution electron micrographs of alginate hydrogels were obtained using a Philips XL30 FEG SEM (Philips, The Netherlands) operating at an accelerating voltage of 5 kV and collecting secondary electron emissions. Samples were crosslinked and dried overnight at 40 °C prior to imaging. Before measurement, they were fixed onto carbon tape and dehydrated in a vacuum chamber. A 5 nm coating of Pt80/Pd20 alloy was then applied via plasma sputtering. The images were taken to assess the homogeneity of the hydrogel surface and to evaluate the ultrastructure of the formulations. Representative micrographs are provided in the supplementary data (Fig. S.1) for reference.

2.4. Measurement of gel fraction and swelling degree

For this test, the hydrogels were first frozen at —20 °C for lyophilization with a Christ freeze-dryer alpha 2–4-LSC (Martin Christ, Germany) for 24 h. Then, to determine the gel fraction (GF), 0.5 × 0.5 cm^2 pieces of lyophilized hydrogel were weighed before (wd_0) swelling in ultrapure water for 120 h. Then, they were lyophilized again and weighted (w_d). From these measurements, the GF was calculated according to Eq. (1),

$$GF = \frac{W_d}{W_{d0}} \tag{1}$$

to quantify the amount of cross-linked polymer chains from the networks. The experiments were performed in quadruplicate.

For the swelling degree, the dry samples weighted for the determination of the GF (w_d), were subsequently immersed for five days at skin temperature (33 °C): once in ultrapure water and a second time in simulated wound fluid (SWF, prepared by mixing maximum recovery diluent (1.037 g/cm^3) with fetal bovine serum (1.012 ± 0.008 g/cm^3) in equal volumes). Afterwards, the swollen hydrogels were removed from solution and weighed (w_s). The swelling degree (SD) was calculated with the Eq. (2),

$$SD\left(\frac{\text{g water}}{\text{g hydrogel}}\right) = \frac{W_s - W_d}{W_d} \text{x} \frac{1}{SG} \tag{2}$$

where the dry weight was corrected by multiplying it first by the GF for the samples submerged in SWF to account for the loss of soluble/non-crosslinked polymer during the swelling process. This correction ensures that the measurement reflects only the material that remains as part of the network. The mass of swollen materials is represented by w_s, w_d is the dry mass, and SG the specific gravity of the applied solution ($SWF_{avg} \approx 1.0245$ g/ml) [11]. This correction accounts for the non-water components of the solution, such as salts and proteins, ensuring the swelling measurement measures only the absorbed liquid. This approach is based on methods reported in earlier literature [17–19]. All experiments were conducted in quadruplicate.

2.5. Measurement of tensile and unconfined compressive strength

Tensile and compression testing were conducted on fresh and 5-day SWF incubated hydrogels using a dynamic mechanic analyzer (DMA) model Q800 (Universal Instruments, USA). For these tests, hydrogels with a methacrylation degree of 11.5 % were made. At least five samples were measured at room temperature in hydrated state for each condition. From both tests, a stress-strain curve was plotted to determine compression (E_c), tensile modulus (E_t), strain-at-break (εB_c, εB_t), compression- (σB_c) and stress-at-break (σB_t) of the hydrogels. The moduli were calculated with the slope of the curve in the elastic deformation zone between 0 and 20 % strain.

For the tensile testing, the specimens were punched out with a custom-made dog bone shape puncher (length = 15 mm, width = 3 mm, gage thickness = 1 mm, total length = 29.5 mm). Double sided tape covered with paper towel was attached to the clamps to prevent the samples from slipping during the test. It was performed until failure at a constant stress-strain rate of 0.050 N/min, an upper force limit of 5 N and a preload force of 1 mN. For compression testing, circular specimens with diameter of 6 mm and thickness of 1 mm were punched and evaluated in a clamp for compression at a constant stress-strain rate of 0.5 N/min until sample failure (cracking followed by fracture) with an upper force limit of 10 N, preload force of 5 mN.

2.6. Cytotoxicity testing

2.6.1. Preparation of scaffolds

The different solutions (ALMA, EGDA, EGDMA, TEGDMA and PETA) were sterile filtered before crosslinking to form the hydrogels with a thickness of 1 mm (as explained in Section 2.3 Crosslinking). Then, fresh circular pieces with a diameter of 3 mm were punched and sterilized with UV at 254 nm by running the preset sterilization program of the biosafety cabinet on each side of the gels. They were rinsed three times with 100 μl of cell culture medium and incubated 24 h at 37 °C, 5 % CO_2 and 90 % RH. The medium was composed of DMEM GlutaMAX™ with 1 μM pyruvate, supplemented with 1 % antibiotic/antimycotic solution and 10 % FBS. Afterwards, the medium was removed, and the hydrogels were ready for the cell-culture experiments.

2.6.2. Hydrogel scaffolds on cell monolayer

NHDF-Ad cultured for two passages in T-175 flasks were seeded in 48-well plates at a density of 4 × 104 cells/cm^2 and allowed to attach overnight. The following day, pre-treated hydrogels were placed in direct contact on top of the cells. This set-up was incubated at 37 °C, 5 % CO_2 and 90 % RH for 7 days. The medium was refreshed every 2–3 days, while leaving the hydrogels intact on top of the cells. During each refreshment, monitoring with an optical microscope Primovert (Zeiss, Germany) was performed.

2.6.3. Cell cytotoxicity

Cell viability was assessed on days 1, 3 and 7. The hydrogels and medium were carefully removed before adding 125 μl of yellow tetrazolium MTT. After a 3 h incubation at 37 °C, 5 % CO2 and 90 % RH, the supernatant was carefully removed, and formazan crystals were extracted by adding 375 μl DMSO for 10 min. Total absorbance at 570 nm of 100 μl of the solubilized product was quantified using SpectraMax ABSPlus microplate reader (Molecular Devices, USA). The experiments were performed with four replicates and the spectrophotometric measurements were done with a technical triplicate.

2.6.4. Cell viability assay

Cell viability was studied on days 1, 3, 5, 6 and 7. Using the LIVE/DEAD Viability/Cytotoxicity Kit L-3224 (Invitrogen, USA). The hydrogels and medium from the well plates were removed and the cells were washed twice with PBS for 5 min. Then, LD solution was added (500 μl per well) and incubated at 37 °C, 5 % CO_2 for 30 min. The staining solution was composed of 2 μM calcein acetoxymethyl ester (ex/em 494/517 nm) and 4 μM ethidium-homodimer-1 (ex/em 528/617 nm) per ml PBS, where the former gives a green signal for live cells due to their intracellular activity, while the latter a red signal for dead cells due to the capacity to enter damaged membranes [20]. Next, two more PBS washes were performed and finally the cells were imaged in the Nikon Eclipse Ti 2 inverted fluorescence microscope. The assay was done in triplicate. Afterwards, the images were processed in triplicate using image J for cell counting, resulting in a semi-quantitative assessment to confirm the results of the MTT assay.

2.7. Statistics

Statistical analysis throughout the research was ran using a two-sample F-test to compare the variances followed by a *t*-test. Statistically significant differences were identified as $p < 0.05$.

3. Results

3.1. Quantification of the methacrylation of sodium alginate

ALMA was acquired through the methacrylation of sodium alginate with methacrylic anhydride. The DS is a resulting parameter that has an important effect on the swelling and mechanical capacity of the cross-linked hydrogels [21]. It is defined as the number of methacrylate moieties introduced relative to the initial amount of hydroxyl functionalities on alginate. This was calculated by applying Eq. (3),

$$DS = \frac{1}{2}\frac{\frac{I_{5.73\ ppm}+I_{6.16\ ppm}}{2}}{I_{4.58\ ppm}+I_{4.97\ ppm}} x100\% \quad (3)$$

based on ^{1}H NMR spectroscopy where the intensities of the characteristic methacrylate alkene peaks (Ha and Hb) present at 5.73 ppm and 6.16 ppm are correlated with alginate's characteristic anomeric carbohydrate signals at 4.58 ppm and 4.97 ppm, respectively the anomeric protons of mannuronic, M-, and glucuronic, G-, residues (H_M and H_G), depicted in Fig. 1. As every monosaccharide unit has two available hydroxyl functionalities for methacrylation, the obtained value is divided by two. The achieved degree of substitution for ALMA was 11,5 % per OH-moiety present in alginate.

ALMA hydrogels were formed by covalent crosslinking based on the reaction of the methacrylate groups in the presence of initiator when exposed to UV light (Fig. 2). Additional covalent crosslinking was achieved by incorporating one of the four crosslinkers: EGDA, EGDMA, TEGDMA, PETA which were assessed to make a comparison study.

3.2. Gel fraction and swelling degree

The hydrogel gel fractions (Fig. 3) were calculated from the dry weight before and after incubation in ultrapure water. Statistical analyses showed differences only between ALMA-EGDMA and EGDA-EGDMA, while no significant differences were found among the other cross-linked hydrogels. In the following step, the swelling capacities were determined after five days of incubation (Fig. 4) to ensure that an equilibrium was reached. While polymerization kinetics and crosslinker structure can influence gelation, the effect of the different crosslinkers became apparent in the swelling behavior rather than in the gel fraction, reflecting differences in network density and structure. Swelling in ultrapure water indicates the maximum material swelling and allows to calculate the gel fraction. In the present case the hydrogels are intended for wound healing applications, so the property is relevant to be translated to the volume of exudate that it could absorb. Therefore, it is performed in a solution that emulates wound fluid (SWF). Overall, the addition of a crosslinker caused a significant reduction on the equilibrium swelling. Significant differences were also found between the different crosslinkers, except for EGDA and EGDMA swollen in SWF, where the difference was not statistically significant.

3.3. Measurement of tensile and compressive strength

The capacity to take up and balance wound fluid is crucial for a material in the wound healing market. However, given exposure to different stresses during use, dressings' mechanical properties are a priority as well. Therefore, E_c, E_t, σB_c, σB_t, εB_c and εB_t were assessed through hydrogel tensile and compressive testing displayed in Fig. 5.

From the obtained data, it can be identified that the hydrogels with EGDA had the highest moduli (around 50 kPa) and stress at break (almost 140 kPa in compression), which outperformed the others. Indeed, the statistical tests ($p < 0.05$) showed stronger hydrogels with EGDA than without it, but also stronger compared to those with EGDMA and PETA. At the same time, EGDA showed a lower maximum strain in tension and compression (51 % and — 35 % respectively) than all other formulations. The least performing hydrogel was EGDMA, given that it was equal or weaker than ALMA and the strain capacity was lower. TEGDMA and PETA showed similar parameters to ALMA, of which moduli were between 10 and 15 kPa, the stress at break 11 and — 80 kPa for tension and compression, with a maximum strain of 60–70 %.

From the obtained data tables (see supplementary data), it can be identified that the hydrogels with EGDA had the highest moduli (around 60 kPa) and σB_c (almost 140 kPa), which outperformed the others.

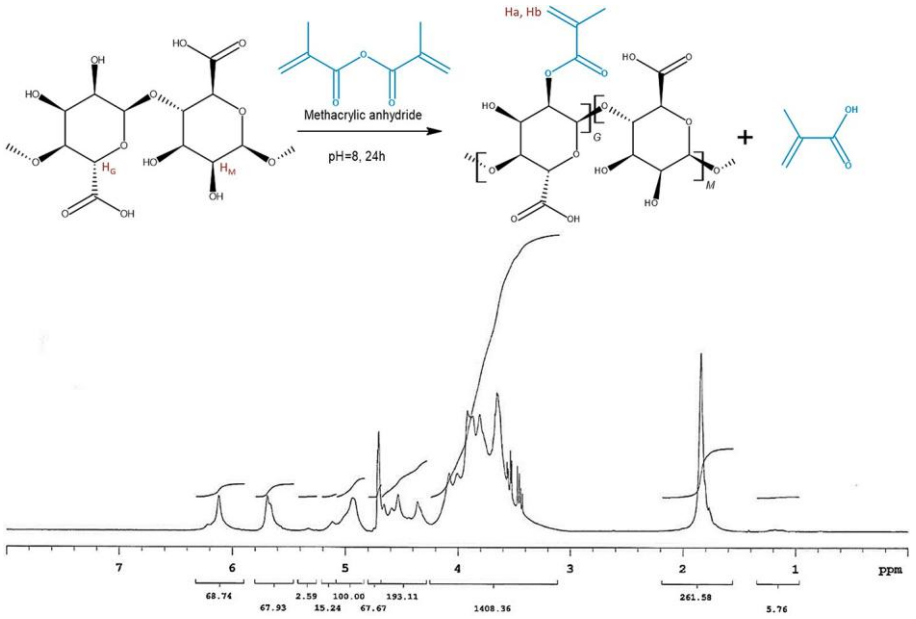

Fig. 1. Alginate methacrylation synthesis of ALMA where the relevant protons for quantification of the degree of modification are highlighted, followed by the ^{1}H NMR spectrum obtained.

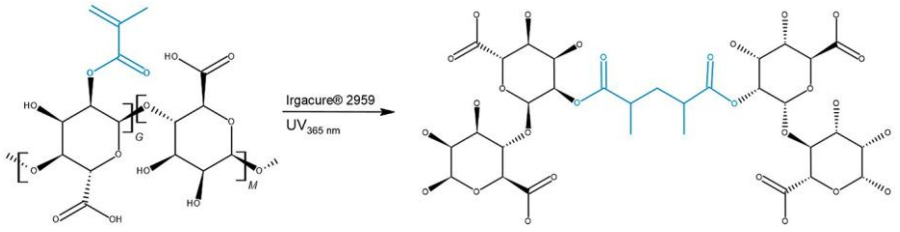

Fig. 2. Methacrylated alginate crosslinking in the presence of Irgacure® 2959 and UV light with a wavelength of 365 nm.

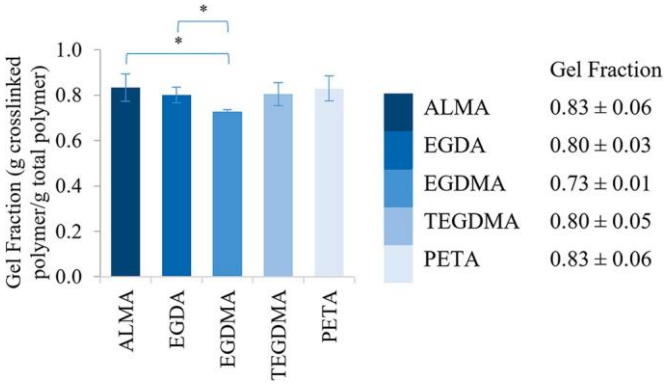

	Gel Fraction
ALMA	0.83 ± 0.06
EGDA	0.80 ± 0.03
EGDMA	0.73 ± 0.01
TEGDMA	0.80 ± 0.05
PETA	0.83 ± 0.06

Fig. 3. Graphical representation (left) and table of values (right) of the gel fraction values obtained for the different crosslinked hydrogels, $n = 4$.

Indeed, the statistical tests ($p < 0.05$) showed stronger hydrogels with EGDA than without it. ALMA's moduli were between 10 and 15 kPa, the σB_t 11 and σB_c — 80 kPa, with ε of 60–70 %. EGDA also proved stronger compared to EGDMA and PETA, but a lower εB_c and εB_t (—35 % and 51 % respectively). The least performing hydrogel was EGDMA, given that it was equal or weaker than ALMA and the strain capacity was lower. While TEGDMA and PETA showed similar parameters. The exact tensile and compressive parameters of the different samples can be consulted in Tables S.1 and S.2 in the supplementary data.

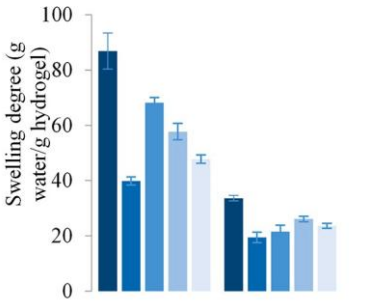

	Ultrapure water	Simulated wound fluid
ALMA	86.9 ± 6.6	33.7 ± 1.0
EGDA	39.9 ± 1.5	19.4 ± 1.9
EGDMA	68.2 ± 1.9	21.5 ± 2.3
TEGDMA	57.7 ± 3.0	26.1 ± 1.0
PETA	47.8 ± 1.5	23.7 ± 0.9

Fig. 4. Graphical representation of the swelling degree after five days incubation in ultrapure water (left) and simulated wound fluid (right) of the different crosslinked hydrogels, n = 4.

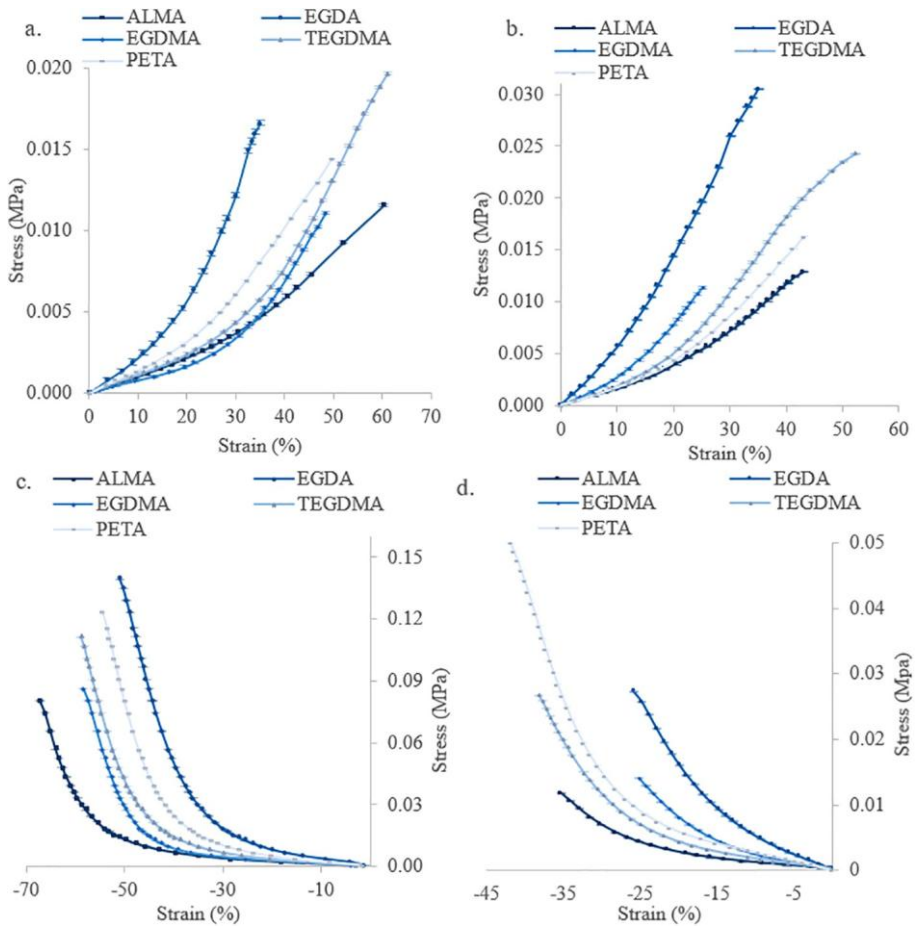

Fig. 5. Tensile (a., b.) and compressive (c., d.) stress-strain curves of the five hydrogels tested. On the left (a., c.), the hydrogels were assessed right after UV crosslinking, while on the right (b., d.) they were evaluated after swelling in simulated wound fluid.

3.4. Confirmation of reactions by Fourier transform infrared spectroscopy

As a qualitative assessment of the chemical structure, functionalization and crosslinking attainment, the materials were characterized by Fourier transform infrared spectroscopy (FTIR), by a Spectrum 100 from PerkinElmer. A representative spectrum of selected materials to compare to the best performing crosslinker are shown in Fig. 6, the characteristic peaks were identified and subsequently summarized in Table 2.

SEM images (Fig. S.1 of supplementary data) showed that both ALMA and EGDA hydrogels exhibited relatively smooth surfaces at lower magnifications (25×). At higher magnifications (100×), the EGDA hydrogel displayed a slightly more granular surface compared to ALMA (B). This morphological difference likely reflects the higher crosslinking density achieved in the presence of EGDA, as also indicated by its lower swelling capacity and superior mechanical strength. EGDA, as a

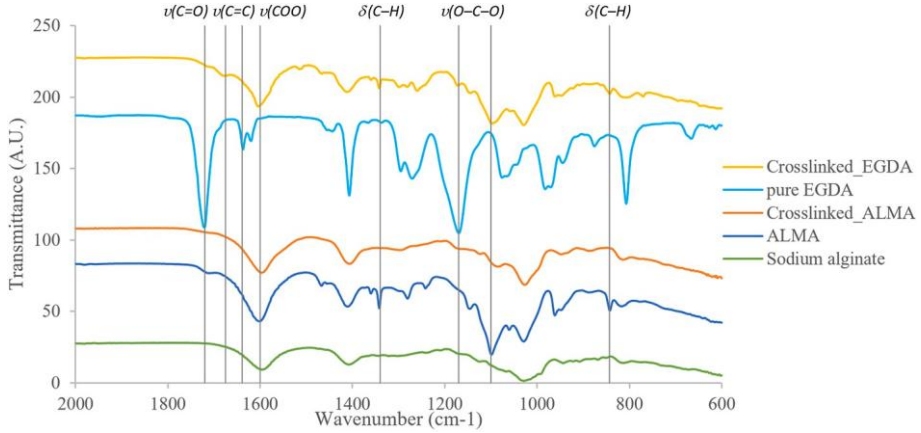

Fig. 6. Fourier transform infrared spectra of sodium alginate prior to modification (green), methacrylated alginate before (dark blue) and after crosslinking (orange), EGDA crosslinker for reference (light blue) and crosslinked ALMA with EGDA as reinforcement (yellow). (For interpretation of the references to colour in this figure legend, the reader is referred to the web *version of this article.)*

Table 2
Relevant characteristic peaks identified in Fig. 6.

Wavenumber (cm^{-1})	Vibration	Strength	Functionality
1720, 1675	ν(C=O)	strong	Ester
1640	ν(C=C)	weak	Alkene
1600	$\nu(COO^{-})$	strong	Carboxylic acid
1350	δ (C–H)	strong	Methyl and methylene
1170, 1100	ν(O–C–O)	strong	Ester
850	δ(C–H)	strong	Vinyl

FTIR spectra of alginate, ALMA, crosslinked ALMA, pure EGDA and crosslinked EGDA.

homobifunctional crosslinker, is known to facilitate efficient network formation through free-radical polymerization. This could have contributed to the increased crosslinking density and the resulting more irregular and rough surface morphology observed in our SEM images [22,23].

3.5. *Cytocompatibility of photocrosslinked alginate hydrogels*

Cytotoxicity testing focused on EGDA-crosslinked hydrogels, as these demonstrated the most favorable balance of mechanical properties and swelling capacity, making them the primary candidate cytocompatibility evaluation. To this end, the metabolic activity and viability of human skin fibroblasts — a cell line directly relevant to wound healing — were assessed using a standard assay widely accepted for the initial biological validation of skin-contact materials [24].

Cells were cultured in direct contact with the hydrogels for 1, 3 and 7 days and were subsequently assessed with a commercial MTT-assay. The cell survival after exposure was calculated by normalizing the absorbance of samples at 490 nm to that of the control without hydrogel (live control). The survival of cells cultured in the presence of hydrogel with crosslinker (112 ± 14 %) was slightly higher than that of cells treated with ALMA hydrogels (98 ± 13 %). However, there was no significant differences in cell viability for all three time periods of culture between the groups exposed to hydrogels and the live control without hydrogel, as shown in Fig. 7. The equivalent dose of pure EGDA applied directly to the cells showed clear toxicity.

Viability was assessed by a Live/Dead assay, a fluorescent staining where live cells are labeled green (calcein AM dye, CA-AM) and dead cells red (ethidium homodimer 1, EthD-1) (Fig. 8). Thereby, inverted microscope and confocal laser scanning microscope observations confirmed the results of the MTT test showing that the hydrogels were non-toxic towards fibroblasts even not after 7 days of exposure and also supported viability. The images present almost no dead cells and there is overall no difference between the treatments and the control (see supplementary data Fig. S.2 for the images on the dead control). Furthermore, the images were processed via image J in triplicate for a semi-quantitative assessment (Fig. 9). This demonstrated no significant difference in the number of live cells over time when exposed to either hydrogel. The dead control, where the cells are expected to die due to a washing step with ethanol, confirmed the growth rate because the count of dead cells (brown line in Fig. 9) followed the same trend as the live cell count. This control is to validate the efficacy of the ethidium homodimer-1 staining.

4. Discussion

ALMA was synthesized by reacting alginate directly with methacrylic anhydride in deionized water. The rate of methacrylic anhydride addition, agitation speed, reaction temperature, pH and other mixing conditions may have particular effects on the reaction quality. An advantage of this synthesis method is that the carboxyl groups on ALMA, remain available for chemical functionalization for further applications [9]. The obtained degree of substitution per repeating unit was 11,5 % per OH-moiety present in alginate. This value is within the range reported in the literature [16,25] and it translates to the crosslinking ability of the network, and the physico-mechanical properties of the formed hydrogels.

A hydrogel's gel fraction gives an indication of the efficiency of a polymer network's crosslinking, representing the proportion of hydrogel that was effectively integrated in the polymer network [26]. In our study, most gel fractions approached or exceeded 80 %, which is considered relatively high for methacrylated biopolymer hydrogels and reflects a generally efficient network formation. However, the limited variation in gel fraction among formulations suggests that the crosslinker type did not strongly determine the final gel fraction under the crosslinking conditions used in this study [27,28]. Nonetheless, the crosslinker will have strong effects on the swelling and mechanical behavior of the formed hydrogels.

The specific threshold for what is considered a high gel fraction can vary depending on the intended application. A gel fraction above 60 % is commonly regarded as sufficient for biopolymer hydrogels to preserve their structural integrity [29]. Hydrogels with higher gel fractions tend to exhibit better mechanical strength and stability, which are desirable for the current application. Nonetheless, as observed in our results, even similar gel fractions, such as the ones obtained here, can lead to different swelling behaviors and mechanical properties, suggesting that factors beyond crosslinking efficiency, including the network structure and material composition, also contribute to the final properties of the hydrogels [30]. Although the polymerization process itself was not the focus of this study, the observed differences in mechanical behavior between hydrogels likely reflect variations in polymerization kinetics and network density specific to each crosslinker.

The reaction of crosslinking agents is complex, it implies different variables such as degree of polymerization, glass transition temperature,

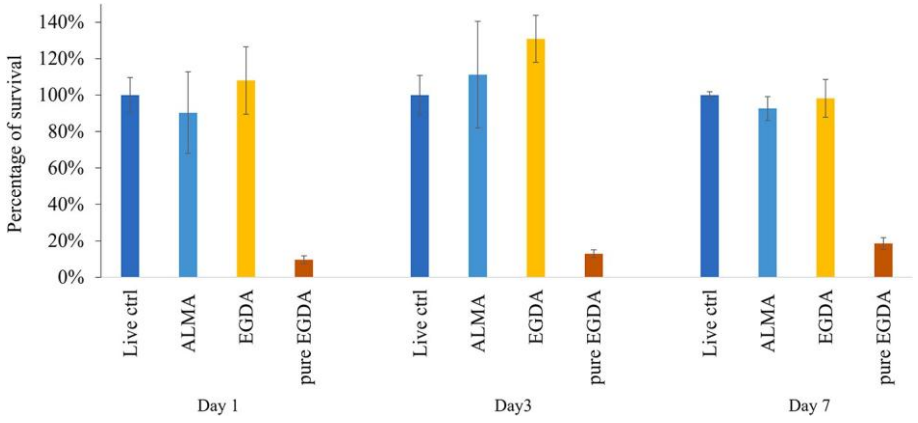

Fig. 7. Survival rate of NHDF-Ad cells cultured in direct contact with hydrogel and pure EGDA for 1, 3 and 7 days (n = 4). Results were obtained with an MTT-assay.

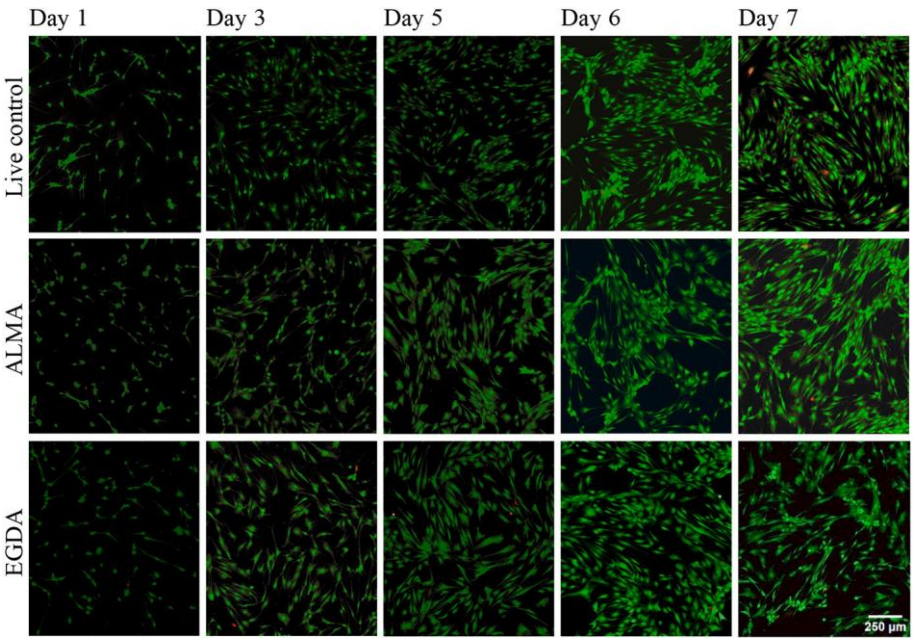

Fig. 8. Viability at 1, 3, 5, 6 and 7 days after application of ALMA and EGDA hydrogels at 37 °C, 90 % RH, 5 % CO_2. Confocal laser scanning microscope images of LIVE/DEAD™ assay on skin fibroblasts (NHDF-Ad). The negative control was culture medium incubated without cells. Test according to ISO 10993-5:2009 standard.

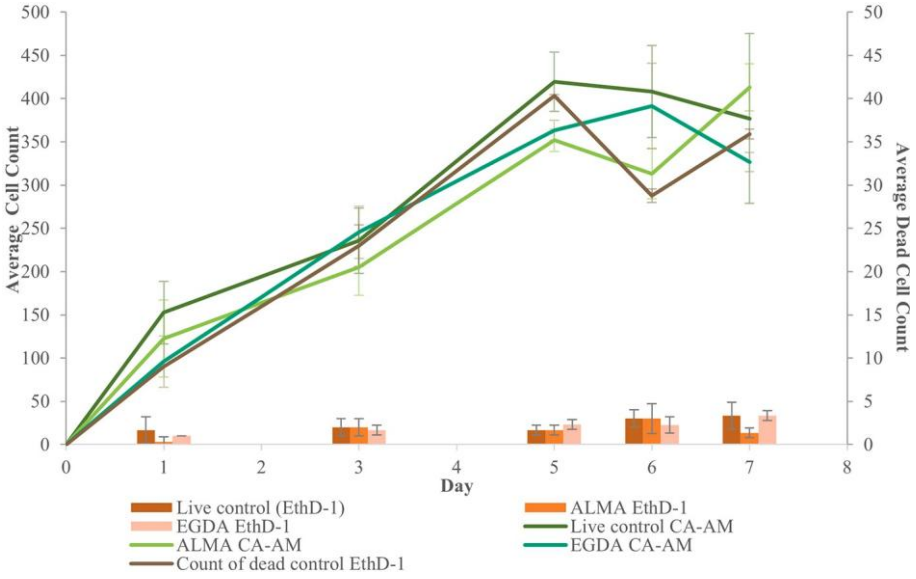

Fig. 9. Cell counting by ImageJ ($n = 3$) of the viability at 1, 3, 5, 6 and 7 days after application of hydrogels at 37 °C, 90 % RH, 5 % CO_2, assessed by Live/Dead assay. Live cells were labeled green (calcein AM dye, CA-AM) and dead cells red (ethidium homodimer 1, EthD-1). (For interpretation of the references to colour in this figure legend, the reader is referred to the web version of this article.)

geometric constraints, and the presence of unreacted molecules [31]. EGDMA is often used for crosslinking due to its short chain, which results in less residual monomer, and it helps increase the resistance to deformation. On the other hand, long chain crosslinkers significantly increase the toughness of hydrogels by introducing flexible segments into the network, which may enhance the material's ability to dissipate energy under stress [32]. However, such effects typically require higher crosslinker concentrations (e.g. ≥15 %) to be significant [33].

It is noteworthy that the sample with EGDMA presented a significantly lower gel fraction compared to the negative control (without additional crosslinker), which may be attributed to the higher steric hindrance introduced by the crosslinker, leading to slower polymerization kinetics, compared to the acrylic counterparts, as reported previously [31]. The lower reactivity of methacrylates compared to acrylates [34–36] further supports the observation that EGDA and PETA showed slightly higher gel fractions. Particularly in the case of PETA, even with a bulkier structure, the steric effect that could be caused may be compensated by the presence of higher and more reactive functionalities (three acrylate groups) than EGDMA, leading to a higher gel fraction [37,38].

In the case of TEGDMA, the longer chain between the functional groups of the polymer could further influence crosslinking efficiency. However, despite these structural differences, none of the other crosslinkers – apart from EGDMA – resulted in a gel fraction statistically different from the control. This indicates that, under the experimental conditions, the crosslinkers, EGDA, TEGDMA and PETA in a 2:1 ratio to

the methacrylic groups in alginate did not strongly affect the final yield of network formation efficiency of the polymeric matrix [14].

The gel fraction values in this study are consistent with current research on methacrylated alginate hydrogels. For instance in a previous study, we reported values up to 89 % for a methacrylated alginate (DS 9 %) crosslinked with acrylic acid and acrylamide [16]. In contrast, hydrogels prepared with a lower degree of methacrylation (DS 6 %) yielded a gel fraction of 66 %, while the present study, using a DS of 11.5 %, achieved higher values [14]. This indicates that degree of methacrylation may remain the primary factor in determining gel fraction, while the choice of crosslinker affects other properties such as network structure, and therefore, resulting performance in swelling and mechanical strength [39].

However, it is important to note that the low swelling observed in EGDMA hydrogels cannot be attributed solely to their lower gel fraction. Rather, the short chain length and less reactive functionality, result in a network that restricts water uptake, despite a lower fraction of polymerized material. In contrast, EGDA, which presented the lowest swelling and highest gel fraction, forms in this case the most efficient and tight network, probably due to a balance of chain length and reactivity.

In an application for wound healing, uptake capacity can be considered high from 30 g fluid absorbed per gram of hydrogel [25,40]. This was achieved by all our different hydrogels, while commercial hydrogels often offer considerably less. For instance, Kaltostat (24.7 ± 1.9 $g_{water}/g_{material}$) and AquacelAg (17.5 ± 1.39 $g_{water}/g_{material}$) are within the reported hydrogels with the highest absorption capacity in ultrapure water [5]. Other formulations such as Hydrosorb and DuoDerm ET absorb as low as 2 to 5 $g_{water}/g_{material}$. Mepilex is another standard wound dressing made of silicone with a swelling capacity of 11.37 ± 0.51. In this sense, there is quite a need of improvement [5]. Overall, in our study the addition of a crosslinker caused a significant reduction on the equilibrium swelling but yet considerably above commercial standards.

The swelling capacity within the different crosslinkers was also significantly different, except for the crosslinkers EGDA and EGDMA in SWF. It is expected that water absorption is reduced when high crosslinking is achieved because a more tightly cross-linked structure with more junction knots per volume unit restrict the fluid absorption capacity [25,29]. However, in our study, EGDMA showed a relatively low gel fraction while also exhibiting a reduced swelling capacity compared to the control hydrogels. This combination suggests that although the crosslinking indicates a lower gel fraction, the resulting network may have lacked the structural stability for the corresponding water uptake [33]. Additionally, this behavior may be influenced by the methacrylate structure itself; the presence of an additional methyl group, when compared to acrylates such as EGDA, could slightly reduce hydrophilicity and affect the network's ability to retain water [41,42]. Nevertheless, the aim of this study was to assess the practical performance of the hydrogels rather than to investigate the underlying polymerization mechanisms. Ultimately, the observed behavior of EGDMA highlights its unsuitability as an additive for this particular application.

In addition, the comparison between EGDMA and TEGDMA highlights interesting differences in swelling behavior depending on the medium used. TEGDMA hydrogels swelled less in ultrapure water than EGDMA, which can be attributed to a longer flexible structure in TEGDMA, possibly leading to an obstruction of initial water uptake. However, contrary to the expectation, when immersed in simulated wound fluid, TEGDMA hydrogels showed higher swelling than EGDMA. This may be related to the proteins and ions in the medium which can interact with each network. Potentially, TEGDMA could expand more under osmotic influence due to its larger, more flexible structure compared to a stiffer EGDMA [33,43]. This difference in swelling behavior underlines the importance of crosslinker selection for tailoring hydrogel handling and performance characteristics, especially in environments simulating physiological conditions.

Furthermore, even when comparable gel fractions were observed, as in the case of PETA and ALMA, a proven difference in swelling was measured. This is likely due to the different molecular structure of the introduced crosslinkers. Having a tri-functional, branched acrylate, PETA lacks the methyl group found in methacrylates, which could contribute to slightly different reactivity, potentially favoring a smaller mesh size in the network, capable of reduced water uptake despite a similar fraction of crosslinked polymer [37,41]. However, it must be taken into consideration that the crosslinker concentration used in this study was deliberately kept at a minimal ratio, increasing it would be expected to significantly amplify the results.

To confirm the suitability of the swelling degree of the other samples, we compared them to other research and found a similar uptake range of methacrylated alginate in various biomedical applications. In bone tissue engineering, it outperforms gelatin with a water uptake from 37 to almost 50 g/g. Chou, et al. obtained 30–45 g/g with photocrosslinked alginate with DS ranging from 3 to 7 % [15]. Water retention by a polymer is highly dependent on its hydrophilicity and microstructure [14]. Due to the presence of the two functional groups: carboxylate and alcohol, alginate is in particular more hydrophilic than other biopolymers often used for the making of wound dressings such as carboxymethylcellulose or gelatin [14,15,25,26]. This has been confirmed in the present study, even after the incorporation of several synthetic crosslinkers.

Regarding the mechanical performance, without a crosslinker, ALMA hydrogels still show a frail strength profile [39]. While it has been shown that with a synthetic approach there is a higher mechanical performance, there are limitations in the properties of swelling and biocompatibility. For instance, oxidized ALMA as a crosslinking spot in poly (ethylene glycol) methacrylate and poly(*N*-hydroxymethyl acrylamide) networks, shows improved toughness and rigidity [9,44]. Another widely studied crosslinker is glutaraldehyde, which allows the formation of a rigid network that can sustain stress of 200 kPa. However, it presents inhomogeneities that result in poor deformability in compression and high-stress at low strain [45]. Thus, the state-of-the-art points towards efforts to improve the mechanical performance without compromising the rest of the properties.

The comparative analysis of tensile and compressive properties revealed that hydrogels crosslinked with EGDA exhibited the highest moduli and stress at break, in both media used for swelling, demonstrating superior mechanical performance among the tested compositions. Regarding swelling in simulated wound fluid, composition-dependent trends were observed. While some samples, such as EGDA-crosslinked hydrogels, maintained or even improved their tensile properties after incubation, others like EGDMA showed reduced mechanical strength. This behavior likely reflects a combination of osmotic effects, ion interactions, and variations in the degree of water uptake in the saline environment of SWF compared to pure water. In particular, the presence of dissolved salts reduces the driving force for swelling, and ionic interactions between the hydrogel matrix and SWF components could alter the polymer chains, leading to either stabilization or softening of the network depending on the crosslinker structure [46]. These observations highlight the importance of the environmental conditions on top of the crosslinker chemistry in determining the final mechanical performance of hydrogels for biomedical applications.

The higher modulus observed in EGDA-containing hydrogels, despite a similar gel fraction to TEGDMA, can be attributed to the shorter chain length of EGDA, leading to a more compact network that increases rigidity, whereas TEGDMA's longer, ethylene glycol segments may permit greater deformation under stress, resulting in lower modulus despite a similar network yield [33]. The comparable mechanical properties observed for TEGDMA and PETA-based hydrogels can be explained by a balance between PETA's highly branched chain, but low ratio used, and TEGDMA's longer chain and lower reactivity [37,41]. This may explain why no further increase in mechanical performance was observed for PETA under the current experimental conditions. These findings were

consistently reflected in the obtained stress-strain values (Tables s.1 and s.2) and confirmed by statistical analysis ($p < 0.05$), confirming the observed trends. Overall, these results emphasize the need to consider both cross-linker structure and the intended application environment when optimizing hydrogel performance.

The mechanical profile of the commercially available products mentioned earlier, Kaltostat, AquacelAg, and Hydrosorb, remains unreported. However, DuoDERM ET and Mepilex have been documented with a Young's modulus of 0.07 ± 0.01 MPa and 0.05 ± 0.00 MPa, respectively [5]. Another commercially used product is fibrin sealants (such as Tisseel®), which are derived from natural polymers and extensively utilized in diverse medical fields, including dermatology [47]. The Young's modulus of these materials has been reported to range from 0.015 to 0.05 MPa, with a maximum tensile strength between 0.029 and 0.08 MPa and an elongation at break spanning 15 % to 60 % [47–49]. These mechanical properties are significantly lower than those of cyanoacrylate-based adhesives, such as Dermabond, which has a standard Young's modulus of approximately 0.050 MPa and is commonly used for skin closure [50]. Furthermore, their compressive modulus is notably low, ranging from 0.002 to 0.007 MPa; however, all parameters can be enhanced up to 30-fold through combinations with different components, such as collagen and glycosaminoglycans [49,51]. Our best formulation, incorporating EGDA, demonstrated superior mechanical performance compared to commercial products DuoDERM ET and Mepilex (synthetic-based on silicone and polyurethane), as it exhibited a similar Young's modulus (~0.06 MPa) while achieving more than twice the swelling capacity (~40 g/g). This result confirms that the reinforcement strategy effectively improved mechanical properties without compromising fluid uptake, maintaining the advantages of a naturally derived approach. Regarding fibrin-based products, their mechanical performance is considerably lower than that of our formulation. However, their intended purpose differs: fibrin is designed to be resorbed by the body and provide adhesion, whereas alginate was selected in the current application specifically for its non-adhesive nature to prevent trauma to newly formed tissue upon dressing removal [52].

Next, the best-performing composition, the one using EGDA as reinforcement, was characterized using infrared absorption spectroscopy. The modification of alginate was confirmed by comparing the spectrum of sodium alginate with that of methacrylated alginate. While successful crosslinking was verified by comparing the spectrum of the crosslinked ALMA hydrogel to that of the uncrosslinked form. Finally, pure EGDA was also measured to identify its specific contributions to the spectrum of the cured hydrogel when the crosslinker was added.

Successful methacrylation was confirmed with the crosslinking capacity of the hydrogel material and the other peaks identified at 850, 1100, 1350, and 1720 cm^{-1} of the FTIR spectra explained in Section 3.4 (Confirmation of reactions by Fourier transform infrared spectroscopy) [53–55]. In our previous research, where acrylic acid and methacrylated alginate were combined, we also found similar characteristic peaks for the same functionalities [16,25]. The expected peak at 1640 cm^{-1} of the carbon-carbon double bond (ν(C=C)) was only appreciable in pure-EGDA and not in the spectrum of ALMA. This is due to the weak nature of the stretch vibration resulting from a slightly polarized C–C bond, in contrast to the nearby presence of the strong carboxylic acid peak resulting from a strongly polarized C–O bond (so with strong dipole moment change during the vibration) in alginate-containing samples at 1600 cm^{-1} [56]. Regarding the crosslinking confirmation, Liguori et al. have also measured a peak around 1700 cm^{-1} attributed to carbonyl and carboxylic moieties of solid-state crosslinked polysaccharides. They highlight that peak intensity may also change according to crosslinking efficiency, but the technique is just qualitative [29]. Finally, the strong stretching vibrations of the ester functionalities (C–O and O–C–O) are clearly visible in both the spectrum of pure EGDA and the spectrum of EGDA-crosslinked ALMA. In contrast, these signals are less pronounced in the spectrum of crosslinked ALMA without EGDA, confirming the presence and structural contribution of EGDA in the cured hydrogel. The next step was to verify the transferability of this high performing formulation in terms of nontoxicity, in order to be applicable for biomedical purposes.

The cell culture tests clearly confirmed viability and nontoxicity in normal human skin fibroblasts. Similar studies of natural-based hydrogels for skin applications have used the same testing such as Lu et al. who used LIVE/DEAD™ cell viability and metabolic activity by MTT assay after 1 and 3 days of treatment with hydrogel extract on NIH-3 T3 mouse fibroblasts. They also found sufficient cytocompatibility, but only up to a determined composition of crosslinking with tilapia skin gelatin [57]. In contrast to our formulation, where we did not find a decrease in viability, other research has reported hydrogels that do present undesirable effects. For instance, carboxymethylcellulose hydrogels loaded with green-synthetized silver nanoparticles for diabetic foot ulcers were assessed on the same cell line (NHDF-Ad) and presented a decrease of viability between 3 and 12 % [58]. Regarding synthetic options, such as glutaraldehyde as a reinforcing agent, it has toxicity concerns due to its functional groups and inflammatory reaction. For this reason, detoxifying strategies have been attempted to increase its application in commercial products [45]. Moreover, ALMA has been added into synthetic systems, such as polyethylene glycol diacrylate-based [59], and proven to somewhat improve cell viability.

Finally, in vitro studies with natural reinforcing agents such as genipin and tannic acid have shown potentially promising results but are still not ready for clinical translation. The former, obtained from the *Gardenia jasminoides* Ellis plant from regions in South Asia is used in traditional medicine due to its excellent biocompatibility and healing promotion. However, the amount required ranges between 5 and 20 wt % [60,61], with an average cost per 100 mg of 200–400€ [62,63], making it extremely unaffordable. On the other hand, tannic acid, which is obtained from the bark of certain trees, is used in a similar proportion to genipin with a significant price reduction (~100€ for 500 g [64]) but its toughening capacity, stability and efficiency is limited [65–67]. Furthermore, the production of commercial fibrin-based materials incurs high costs due to stringent quality control measures required to mitigate already minimal risks of infectious disease transmission, as well as the complex purification steps necessary for their manufacture [52]. In contrast, the EGDA in our formulation is in a moderate price range of around 100€ for 5 ml in high purity [68], but it is required in an amount as low as 0.1 wt% for the desired effects. Considering this, our hydrogel proposes a convenient compromise of physico-mechanical properties and cost, with no sacrifice of biocompatibility; contributing to the struggle of finding the appropriate material for reinforcement hydrogel wound dressings.

5. Conclusions

In summary, EGDA proved to be a promising reinforcing agent for wound dressings in low concentration (molar ratio addition of (meth) acrylate functionalities 2:1 EGDA:ALMA). Our natural-based hydrogel exhibited a competitive performance for the market taking the current state of the art research and commercial product availability into account. The mechanically enhanced hydrogels showed outperforming wound fluid absorption capacity and proved biocompatible despite the presence of synthetic acrylic groups. It is indeed a viable and cost-effective crosslinker for enhancing natural-based hydrogels, due to availability and minimal amount required (the molar ratio corresponds to ~0.1 wt%). To further develop our platform, it will be necessary to incorporate active compounds that contribute to the healing process, for instance with antibacterial properties or regulation of the immune response. Related tests will include the assessment of antioxidant, anti-inflammatory and antimicrobial activity, as well as the scratch assay to measure wound closure rate as an indication of favorable wound healing followed by in vivo testing.

Funding

FWO-SB 1S33424N and FWO Project G07562.

CRediT authorship contribution statement

Carolina Gutierrez Cisneros: Writing – review & editing, Writing – original draft, Visualization, Validation, Project administration, Methodology, Investigation, Funding acquisition, Formal analysis, Data curation, Conceptualization. **Hannah Agten:** Writing – review & editing, Visualization, Supervision, Methodology, Formal analysis, Conceptualization. **Elien Derveaux:** Validation, Investigation, Formal analysis, Data curation. **Peter Adriaensens:** Writing – review & editing, Validation, Supervision, Investigation, Formal analysis. **Veerle Bloemen:** Writing – review & editing, Supervision, Methodology, Conceptualization. **Arn Mignon:** Writing – review & editing, Supervision, Resources, Project administration, Methodology, Funding acquisition, Formal analysis, Conceptualization.

Declaration of competing interest

The authors declare that they have no known competing financial interests or personal relationships that could have appeared to influence the work reported in this paper.

Acknowledgments

Financial support from Hasselt University and the Research Foundation Flanders (FWO Vlaanderen) via the Hercules project (AUHL/15/2-GOH3816N) is gratefully acknowledged.

Appendix A. Supplementary data

Supplementary data to this article can be found online at https://doi.org/10.1016/j.reactfunctpolym.2025.106330.

Data availability

The processed data required to reproduce the above findings are within the article and its supplementary materials.

References

[1] K. Varaprasad, T. Jayaramudu, V. Kanikireddy, C. Toro, E.R. Sadiku, Alginate-based composite materials for wound dressing application: a mini review, Carbohydr. Polym. 236 (2020) 116025, https://doi.org/10.1016/J.CARBPOL.2020.116025.

[2] F. Abasalizadeh, S.V. Moghaddam, E. Alizadeh, E. Akbari, E. Kashani, S.M. B. Fazljou, M. Torbati, A. Akbarzadeh, Alginate-based hydrogels as drug delivery vehicles in cancer treatment and their applications in wound dressing and 3D bioprinting, J. Biol. Eng. 14 (2020) 1–22, https://doi.org/10.1186/S13036-020-0227-7.

[3] J. Hoque, R.G. Prakash, K. Paramanandham, B.R. Shome, J. Haldar, Biocompatible injectable hydrogel with potent wound healing and antibacterial properties, Mol. Pharm. 14 (2017) 1218–1230, https://doi.org/10.1021/acs.molpharmaceut.6b01104.

[4] E.J. Britto, T.A. Nezwek, P. Popowicz, M. Robins, Wound Dressings, Techniques in Small Animal Wound Management, 2024, pp. 127–154, https://doi.org/10.1002/9781119933861.ch8.

[5] M. Minsart, S. Van Vlierberghe, P. Dubruel, A. Mignon, Commercial wound dressings for the treatment of exuding wounds: an in-depth physico-chemical comparative study, Burns Trauma 10 (2022), https://doi.org/10.1093/BURNST/TKAC024.

[6] J. Qin, M. Li, M. Yuan, X. Shi, J. Song, Y. He, H. Mao, D. Kong, Z. Gu, Gallium(III)-mediated dual-cross-linked alginate hydrogels with antibacterial properties for promoting infected wound healing, ACS Appl. Mater. Interfaces 14 (2022), https://doi.org/10.1021/ACSAMI.2C02497.

[7] M. Dattilo, F. Patitucci, S. Prete, O.I. Parisi, F. Puoci, Polysaccharide-based hydrogels and their application as drug delivery systems in cancer treatment: a review, J. Funct. Biomater. 14 (2023), https://doi.org/10.3390/JFB14020055.

[8] J. Tan, Y. Luo, Y. Guo, Y. Zhou, X. Liao, D. Li, X. Lai, Y. Liu, Development of alginate-based hydrogels: crosslinking strategies and biomedical applications, Int. J. Biol. Macromol. 239 (2023) 124275, https://doi.org/10.1016/J.IJBIOMAC.2023.124275.

[9] M. Hasany, S. Talebian, S. Sadat, N. Ranjbar, M. Mehrali, G.G. Wallace, M. Mehrali, Synthesis, properties, and biomedical applications of alginate methacrylate (ALMA)-based hydrogels: current advances and challenges, Appl. Mater. Today 24 (2021) 101150, https://doi.org/10.1016/J.APMT.2021.101150.

[10] A. Ajam, Y. Huang, M.S. Islam, K.A. Kilian, J.J. Kruzic, Mechanical and biological behavior of double network hydrogels reinforced with alginate versus gellan gum, J. Mech. Behav. Biomed. Mater. 157 (2024) 106642, https://doi.org/10.1016/J.JMBBM.2024.106642.

[11] A. Bucciarelli, C. Zhao, X. Bai, R. Kay, A. Latif, K.J. Williams, A. Tirella, Exploiting response surface methodology to engineer the mechanical properties of alginate-based hydrogels, Macromol. Mater. Eng. 310 (2025) 2400296, https://doi.org/10.1002/MAME.202400296.

[12] M. Mohamadhoseini, Z. Mohamadnia, Alginate-based self-healing hydrogels assembled by dual cross-linking strategy: fabrication and evaluation of mechanical properties, Int. J. Biol. Macromol. 191 (2021) 139–151, https://doi.org/10.1016/J.IJBIOMAC.2021.09.062.

[13] Y. Gao, X. Geng, X. Wang, N. Han, X. Zhang, W. Li, Synthesis and characterization of microencapsulated phase change materials with chitosan-based polyurethane shell, Carbohydr. Polym. 273 (2021) 118629, https://doi.org/10.1016/J.CARBPOL.2021.118629.

[14] J. Lewandowska-Łan´cucka, K. Mystek, A. Mignon, S. Van Vlierberghe, A. Łatkiewicz, M. Nowakowska, Alginate- and gelatin-based bioactive photocross-linkable hybrid materials for bone tissue engineering, Carbohydr. Polym. 157 (2017) 1714–1722, https://doi.org/10.1016/J.CARBPOL.2016.11.051.

[15] A.I. Chou, S.B. Nicoll, Characterization of photocrosslinked alginate hydrogels for nucleus pulposus cell encapsulation, J. Biomed. Mater. Res. A 91 (2009) 187–194, https://doi.org/10.1002/JBM.A.32191.

[16] A. Mignon, J. Vermeulen, G.J. Graulus, J. Martins, P. Dubruel, N. De Belie, S. Van Vlierberghe, Characterization of methacrylated alginate and acrylic monomers as versatile SAPs, Carbohydr. Polym. 168 (2017) 44–51, https://doi.org/10.1016/J.CARBPOL.2017.03.040.

[17] G.J. Graulus, A. Mignon, S. Van Vlierberghe, H. Declercq, K. Fehe´r, M. Cornelissen, J.C. Martins, P. Dubruel, Cross-linkable alginate-graft-gelatin copolymers for tissue engineering applications, Eur. Polym. J. 72 (2015) 494–506, https://doi.org/10.1016/J.EURPOLYMJ.2015.06.033.

[18] A. Mignon, D. Snoeck, D. Schaubroeck, N. Luickx, P. Dubruel, S. Van Vlierberghe, N. De Belie, pH-responsive superabsorbent polymers: a pathway to self-healing of mortar, React. Funct. Polym. 93 (2015) 68–76, https://doi.org/10.1016/J.REACTFUNCTPOLYM.2015.06.003.

[19] N.R. Richbourg, M. Wancura, A.E. Gilchrist, S. Toubbeh, B.A.C. Harley, E. Cosgriff-Hernandez, N.A. Peppas, Precise control of synthetic hydrogel network structure via linear, independent synthesis-swelling relationships, Sci. Adv. 7 (2021) eabe3245, https://doi.org/10.1126/SCIADV.ABE3245.

[20] Scientific TermoFisher, LIVE/DEAD™ Viability/Cytotoxicity Kit, for Mammalian Cells. https://www.thermofisher.com/order/catalog/product/L3224, 2024.

[21] P. Wu, Y. Fang, K. Chen, M. Wu, W. Zhang, S. Wang, D. Liu, J. Gao, H. Li, J. Lv, Y. Zhao, Study of double network hydrogels based on sodium methacrylate alginate and carboxymethyl chitosan, Eur. Polym. J. 194 (2023) 112137, https://doi.org/10.1016/J.EURPOLYMJ.2023.112137.

[22] E. Olaret, B. Balanuca, J. Ghitman, I.C. Stancu, A. Serafim, Reinforcement of nanostructured polyacrylamide hydrogels through the generation of secondary physical network using the nanoparticles' functional groups, Polym. Test. 132 (2024) 108380, https://doi.org/10.1016/J.POLYMERTESTING.2024.108380.

[23] R.A. Scott, N.A. Peppas, Highly crosslinked, PEG-containing copolymers for sustained solute delivery, Biomaterials 20 (1999) 1371–1380, https://doi.org/10.1016/S0142-9612(99)00040-X.

[24] K.K. Kłosin´ski, R.A. Wach, M.K. Girek-Bąk, B. Rokita, D. Kołat, Z˙. Kałuzin´ska-Kołat, B. Kłosin´ska, Ł. Duda, Z.W. Pasieka, Biocompatibility and mechanical properties of carboxymethyl chitosan hydrogels, Polymers 15 (2023) 144, https://doi.org/10.3390/POLYM15010144/S1.

[25] M. Minsart, A. Mignon, A. Arslan, I.U. Allan, S. Van Vlierberghe, P. Dubruel, M. Minsart, A. Mignon, A. Arslan, S. Van Vlierberghe, P. Dubruel, I.U. Allan, Activated carbon containing PEG-based hydrogels as novel candidate dressings for the treatment of malodorous wounds, Macromol. Mater. Eng. 306 (2021) 2000529, https://doi.org/10.1002/MAME.202000529.

[26] O.M. Ionescu, A. Mignon, M. Minsart, J. Van Hoorick, I. Gardikiotis, I.D. Caruntu, S.E. Giusca, S. Van Vlierberghe, L. Profire, Gelatin-based versus alginate-based hydrogels: providing insight in wound healing potential, Macromol. Biosci. 21 (2021) 2100230, https://doi.org/10.1002/MABI.202100230.

[27] Y. Zhao, J. Zhou, H. Zhang, X. Liang, Chen, H. Tan, L. Zhao, Y. Zhou, J. Zhang, H. Liang, X. Chen, H. Tan, Natural polymer-based hydrogels: from polymer to biomedical applications, Pharmaceutics 15 (2023) 2514, https://doi.org/10.3390/PHARMACEUTICS15102514.

[28] H. Ma, Y. Peng, S. Zhang, Y. Zhang, P. Min, Effects and progress of photo-crosslinking hydrogels in wound healing improvement, Gels 8 (2022) 609, https://doi.org/10.3390/GELS8100609.

[29] A. Liguori, L. Paltrinieri, A. Stancampiano, C. Gualandi, M. Gherardi, V. Colombo, M.L. Focarete, Solid-state crosslinking of polysaccharide electrospun fibers by atmospheric pressure non-equilibrium plasma: a novel straightforward approach, Plasma Process. Polym. 12 (2015) 1195–1199, https://doi.org/10.1002/PPAP.201500054.

[30] E. Budianto, A. Amalia, Swelling behavior and mechanical properties of chitosan-poly(N-vinyl-pyrrolidone) hydrogels, J. Polym. Eng. 40 (2020) 551–560, https://doi.org/10.1515/POLYENG-2019-0169.

[31] Z. Veli˘ci´c, J. Rusmirovi´c, N. Prlainovi´c, N. Tomi´c, Z. Veli˘ckovi´c, K. Taleb, A. D. Marinkovi´c, The optimization of glycidyl methacrylate based terpolymer monolith synthesis: an effective Candida rugosa lipase immobilization support, J. Polym. Res. 27 (2020) 1–16, https://doi.org/10.1007/S10965-020-02127-Z.
[32] Z. Guo, X. Lu, X. Wang, X. Li, J. Li, J. Sun, Z. Guo, X. Lu, X. Wang, X. Li, J. Li, J. Sun, Engineering of chain rigidity and hydrogen bond cross-linking toward ultra-strong, healable, recyclable, and water-resistant elastomers, Adv. Mater. 35 (2023) 2300286, https://doi.org/10.1002/ADMA.202300286.
[33] G. Ceylan, S. Emik, T. Yalcinyuva, E. Sunbulog˘lu, E. Bozdag, F. Unalan, The effects of cross-linking agents on the mechanical properties of poly (methyl methacrylate) resin, Polymers 15 (2023) 2387, https://doi.org/10.3390/POLYM15102387/S1.
[34] O.R. Monaghan, S.T. Skowron, J.C. Moore, M. Pin-No´, K. Kortsen, R.L. Atkinson, E. Krumins, J.C. Lentz, F. Machado, Z. Onat, A. Brookfield, D. Collison, A. N. Khlobystov, D. De Focatiis, D.J. Irvine, V. Taresco, R.A. Stockman, S.M. Howdle, A self-crosslinking monomer, α-pinene methacrylate: understanding and exploiting hydrogen abstraction, Polym. Chem. 13 (2022) 5557–5567, https://doi.org/10.1039/D2PY00878E.
[35] N. Dei, K. Ishihara, A. Matsumoto, C. Kojima, Preparation and characterization of acrylic and methacrylic phospholipid-mimetic polymer hydrogels and their applications in optical tissue clearing, Polymers 16 (2024) 241, https://doi.org/10.3390/POLYM16020241/S1.
[36] S. Shukla, J.S.P. Rai, Synthesis and kinetic study of diacrylate and dimethacrylate, Int. J. Plast. Technol. 17 (2013) 182–193, https://doi.org/10.1007/S12588-013-9058-4.
[37] R.S.H. Wong, M. Ashton, K. Dodou, Effect of crosslinking agent concentration on the properties of unmedicated hydrogels, Pharmaceutics 7 (2015) 305–319, https://doi.org/10.3390/PHARMACEUTICS7030305.
[38] A. Shikanov, R.M. Smith, M. Xu, T.K. Woodruff, L.D. Shea, Hydrogel network design using multifunctional macromers to coordinate tissue maturation in ovarian follicle culture, Biomaterials 32 (2011) 2524–2531, https://doi.org/10.1016/J.BIOMATERIALS.2010.12.027.
[39] O. Jeon, K.H. Bouhadir, J.M. Mansour, E. Alsberg, Photocrosslinked alginate hydrogels with tunable biodegradation rates and mechanical properties, Biomaterials 30 (2009) 2724–2734, https://doi.org/10.1016/J.BIOMATERIALS.2009.01.034.
[40] M. Uzun, S.C. Anand, T. Shah, In vitro characterisation and evaluation of different types of wound dressing materials, journal of biomedical, Eng. Technol. 1 (2013) 1–7, https://doi.org/10.12691/jbet-1-1-1.
[41] G. Odian, Radical chain polymerization, in: Principles of Polymerization, Fourth ed., John Wiley & Sons, Ltd, 2004, pp. 198–349, https://doi.org/10.1002/047147875X.CH3.
[42] F.A. Plamper, W. Richtering, Functional microgels and microgel systems, Acc. Chem. Res. 50 (2017) 131–140, https://doi.org/10.1021/acs.accounts.6b00544.
[43] S. Keten, F. Go¨nülkirmaz, P. Karacan, D. Ceylan, S. Abdurrahmanog˘lu, Synergetic effect of the crosslinker size and polysaccharide type on the acrylamide networks, J. Appl. Polym. Sci. 141 (2024) e55900, https://doi.org/10.1002/APP.55900.
[44] P. Zorlutuna, J.H. Jeong, H. Kong, R. Bashir, Stereolithography-based hydrogel microenvironments to examine cellular interactions, Adv. Funct. Mater. 21 (2011) 3642–3651, https://doi.org/10.1002/ADFM.201101023.
[45] G. Mugnaini, R. Gelli, L. Mori, M. Bonini, How to cross-link gelatin: the effect of glutaraldehyde and glyceraldehyde on the hydrogel properties, ACS Appl. Polym. Mater. 5 (2023) 9192–9202, https://doi.org/10.1021/acsapm.3c01676.
[46] J. Li, D.J. Mooney, Designing hydrogels for controlled drug delivery, Nat. Rev. Mater. 12 (1) (2016) 1–17, https://doi.org/10.1038/natrevmats.2016.71.
[47] A. Amirhekmat, W.E. Brown, E.Y. Salinas, J.C. Hu, K.A. Athanasiou, D. Wang, Mechanical evaluation of commercially available fibrin sealants for cartilage repair, Cartilage 15 (2023) 147, https://doi.org/10.1177/19476035231163273.
[48] W.L. Hickerson, I. Nur, R. Meidler, A comparison of the mechanical, kinetic, and biochemical properties of fibrin clots formed with two different fibrin sealants, Blood Coagul. Fibrinolysis 22 (2011) 19–23, https://doi.org/10.1097/MBC.0B013E32833FCBFB.
[49] J.A. Rojas-Murillo, M.A. Simental-Mendía, N.K. Moncada-Saucedo, P. Delgado-Gonzalez, J.F. Islas, J.A. Roacho-P´erez, E.N. Garza-Trevin˜o, Physical, mechanical, and biological properties of fibrin scaffolds for cartilage repair, Int. J. Mol. Sci. 23 (2022) 9879, https://doi.org/10.3390/IJMS23179879.
[50] A.J. Singer, L. Perry, A comparative study of the surgically relevant mechanical characteristics of the topical skin adhesives, Acad. Emerg. Med. 19 (2012) 1281–1286, https://doi.org/10.1111/ACEM.12009.
[51] T.N. Snyder, K. Madhavan, M. Intrator, R.C. Dregalla, D. Park, A fibrin/hyaluronic acid hydrogel for the delivery of mesenchymal stem cells and potential for articular cartilage repair, J. Biol. Eng. 8 (2014) 1–11, https://doi.org/10.1186/1754-1611-8-10.
[52] E. Anitua, A. Pino, R. Prado, F. Muruzabal, M.H. Alkhraisat, Biochemical and biomechanical characterization of an autologous protein-based fibrin sealant for regenerative medicine, J. Mater. Sci. Mater. Med. 35 (2024) 1–12, https://doi.org/10.1007/S10856-024-06780-4.
[53] B.H. Stuart, Infrared Spectroscopy: Fundamentals and Applications, 2005, pp. 1–224, https://doi.org/10.1002/0470011149.
[54] C. Mahapatra, G.Z. Jin, H.W. Kim, Alginate-hyaluronic acid-collagen composite hydrogel favorable for the culture of chondrocytes and their phenotype maintenance, Tissue Eng. Regen. Med. 13 (2016) 538–546, https://doi.org/10.1007/S13770-016-0059-1.
[55] O. Jeon, D.S. Alt, S.M. Ahmed, E. Alsberg, The effect of oxidation on the degradation of photocrosslinkable alginate hydrogels, Biomaterials 33 (2012) 3503–3514, https://doi.org/10.1016/J.BIOMATERIALS.2012.01.041.
[56] Q.F. Li, K. Lu, Q. Zhou, D.H. Baik, A study on interfacial mechanisms and structure of poly(ethylene-co- methacrylic acid)/copper with reflection-absorption infrared spectroscopy, J. Mater. Sci. 41 (2006) 8271–8275, https://doi.org/10.1007/S10853-006-1006-7.
[57] Y. Lu, M. Zhao, Y. Peng, S. He, X. Zhu, C. Hu, G. Xia, T. Zuo, X. Zhang, Y. Yun, W. Zhang, X. Shen, A physicochemical double-cross-linked gelatin hydrogel with enhanced antibacterial and anti-inflammatory capabilities for improving wound healing, J. Nanobiotechnol. 20 (2022) 1–26, https://doi.org/10.1186/S12951-022-01634-Z.
[58] M. Ruffo, O.I. Parisi, M. Dattilo, F. Patitucci, R. Malivindi, V. Pezzi, T. Tzanov, F. Puoci, Synthesis and evaluation of wound healing properties of hydro-diab hydrogel loaded with green-synthetized AGNPS: in vitro and in ex vivo studies, Drug Deliv. Transl. Res. 12 (2022) 1881, https://doi.org/10.1007/S13346-022-01121-W.
[59] C. Cha, S.Y. Kim, L. Cao, H. Kong, Decoupled control of stiffness and permeability with a cell-encapsulating poly(ethylene glycol) dimethacrylate hydrogel, Biomaterials 31 (2010) 4864–4871, https://doi.org/10.1016/J.BIOMATERIALS.2010.02.059.
[60] Y. Yu, S. Xu, S. Li, H. Pan, Genipin-cross-linked hydrogels based on biomaterials for drug delivery: a review, Biomater. Sci. 9 (2021) 1583–1597, https://doi.org/10.1039/D0BM01403F.
[61] P. Sapuła, K. Bialik-Wąs, K. Malarz, Are natural compounds a promising alternative to synthetic cross-linking agents in the preparation of hydrogels? Pharmaceutics 15 (2023) 253 https://doi.org/10.3390/PHARMACEUTICS15010253.
[62] Sigma Aldrich, Genipin Powder. https://www.sigmaaldrich.com/BE/en/product/sigma/g4796, 2024 (accessed September 19, 2024).
[63] MedChemExpress, Genipin, Crosslinking Reagent. https://www.medchemexpress.com/Genipin.html, 2024 (accessed September 19, 2024).
[64] ACS, Tannic Acid. https://www.sigmaaldrich.com/BE/en/product/sial/403040?utm_source=google&utm_medium=cpc&utm_campaign=10640610204&utm_content=105212359676&gclid=CjwKCAjwl6-3BhBWEiwApN6_kha9Zr43pl8QXByNLIc6hOPzaDbM9m5KkSuFNtfb4r_SIOiNCIXv0xoCpcEQAvD_BwE, 2024 (accessed September 20, 2024).
[65] C. Chen, H. Yang, X. Yang, Q. Ma, Tannic acid: a crosslinker leading to versatile functional polymeric networks: a review, RSC Adv. 12 (2022) 7689–7711, https://doi.org/10.1039/D1RA07657D.
[66] A. Oryan, A. Kamali, A. Moshiri, H. Baharvand, H. Daemi, Chemical crosslinking of biopolymeric scaffolds: current knowledge and future directions of crosslinked engineered bone scaffolds, Int. J. Biol. Macromol. 107 (2018) 678–688, https://doi.org/10.1016/J.IJBIOMAC.2017.08.184.
[67] Z. Xu, Y. Chen, Y. Cao, B. Xue, Tough hydrogels with different toughening mechanisms and applications, Int. J. Mol. Sci. 25 (2024) 2675, https://doi.org/10.3390/IJMS25052675.
[68] Thermo Scientific Chemicals, Ethylene Diacrylate. https://www.thermofisher.com/order/catalog/product/366970050, 2024. (Accessed 20 September 2024).